A convex optimisation-based approach to detect and estimate manoeuvres

Laura Pirovano *[1] and Roberto Armellin †[1]

[1]Te Pūnaha Ātea – Space Institute, University of Auckland, New Zealand

1 Introduction

Since the advent of the space era, the number of resident space objects (RSOs) has grown and with it the problem of accurately determining their state. This is fundamental to maintain a collision-free environment in space, predict space events and perform activities. One of the many tasks pertaining to space situational awareness (SSA) is thus to build and maintain a catalogue of RSOs. While building the catalogue, it is important to associate multiple observations to the same object to perform orbit determination (OD) and improve the orbit's knowledge [1, 2]. To maintain the catalogue, RSOs need to be timely re-observed and the new observations need to be statistically compatible with the known object. Most association routines assume natural motion of the body in between observations, with association metrics deciding whether observations belong to the same RSO. However, active RSOs may perform manoeuvres which are not included in the dynamical model used for association. This mismodelling deteriorates the association routine, creating a mismatch where on the one hand an unknown RSO is detected - the new observation - and on the other hand a known object stops being updated - the spacecraft before the manoeuvring event. This paper outlines a new step to be added to the catalogue maintenance where a manoeuvre profile is estimated to connect two otherwise uncorrelated orbits and recover the association.

2 Problem formulation

In order to make the description clearer, refer to fig. 1 for the following paragraph. Suppose two states - the outcome of an OD - are available at two epochs t_0 and t_1, simplified with a black dot and a shaded ellipse, $(\mathbf{X}_{0,0}, \Sigma_{0,0})$, $(\mathbf{X}_{1,1}, \Sigma_{1,1})$. The state at the earliest epoch is propagated forward to the second one, determining a reference trajectory, the white line with black squares, $(\mathbf{X}_{0,1}, \Sigma_{0,1})$. The propagated and determined states will not correlate with typical data association techniques [3, 4, 1], but correlation may be recovered assuming a manoeuvre has happened. The proposed methodology considers the implementation of an impulsive maneuver $\Delta\mathbf{v}_i$ at every node in which the reference trajectory is discretised $i \in [0, N]$, the black squares, where $i = 0$ coincides with t_0 and $i = N$ with t_1.

State transition matrices (STMs) $\left(M_i \in \mathbb{R}^{6x3}\right)$ are used to map these maneuvers' effects forward in time, as shown by the red and green dashes. For example, a manoeuvre performed at node i will be mapped at node $j > i$ with

$$\Delta\mathbf{X}_{j,\delta\mathbf{v}_i} = \left[\prod_{k=i}^{j} M_{k,i}\right] \Delta\mathbf{v}_i. \tag{1}$$

The final deviation due to the cumulative effect of all manoeuvres until t_1 is then:

$$\Delta\mathbf{X}_{1,\delta\mathbf{v}} = \sum_{i=0}^{N} \left[\prod_{k=i}^{N} M_{k,i}\right] \Delta\mathbf{v}_i. \tag{2}$$

STMs $\left(R_i \in \mathbb{R}^{6x6}\right)$ are also used to map a deviation $\Delta\mathbf{X}_0$ in the initial state forward in time (blue dashes):

$$\Delta\mathbf{X}_{1,\delta X_0} = \prod_{k=0}^{N} \left(R_k\right) \Delta\mathbf{X}_0. \tag{3}$$

The cumulative effect of all manoeuvres and initial deviation allows the state at t_1 to reach the desired location.

The goal is to find the trajectory with the least amount of propellant used:

$$\min \sum_{i=0}^{N} \|\delta\mathbf{v}_i\|, \tag{4}$$

having the $\delta\mathbf{v}$ components at each node, the state at each node $\mathbf{X}$, and the initial and final deviations $\delta\mathbf{X}_0, \delta\mathbf{X}_1$ as optimisation variables ($9N + 12$ variables), meeting the following constraints:

- maximum Δv at each node (which defines the impulsive or low-thrust nature of the maneuver)

$$\|\delta\mathbf{v}_i\| \leq \Delta v_M \quad \forall i \in \{1, \ldots, N\} \tag{5}$$

*Email: laura.pirovano@auckland.ac.nz
†Email: roberto.armellin@auckland.ac.nz

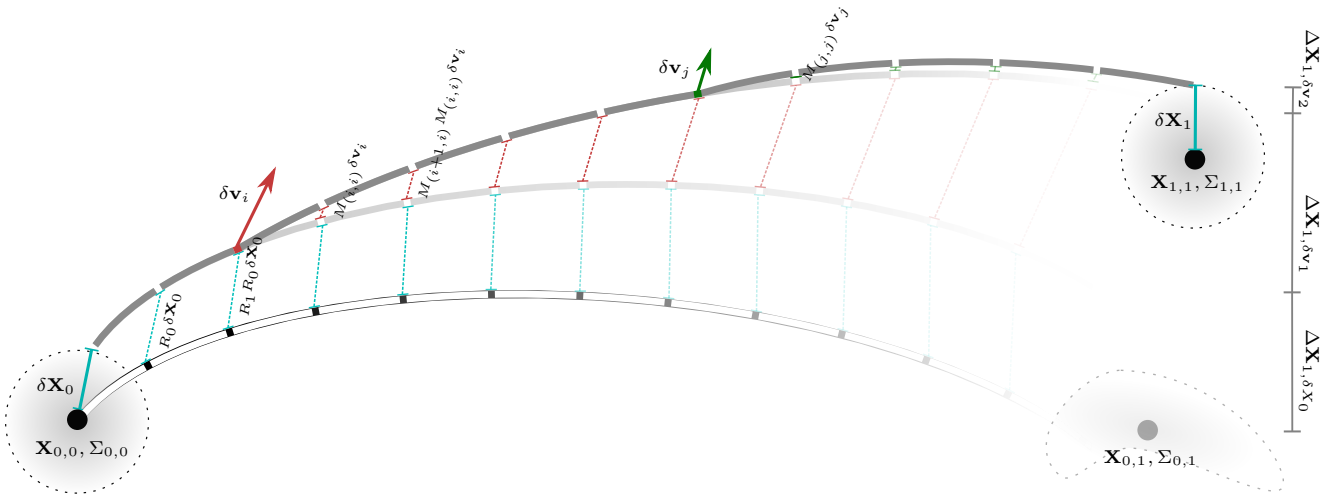

Figure 1: Initial trajectory and linear influence of initial deviation and mid-course manoeuvres to match final deviation.

- maximum variation on initial and final states to account for the OD uncertainty, in the form the Mahalanobis distance, through a chi-square quantile with confidence level α:

$$\frac{1}{2}\delta\mathbf{X}_j^T\Sigma_{(j,j)}\delta\mathbf{X}_j \leq q_{\chi^2}(\alpha,6) = \mathcal{M} \quad j=0,1 \quad (6)$$

- continuity of the trajectory, where $\tilde{\mathbf{X}}_i$ is the initially propagated state at node i while $\mathbf{X}_i$ is the state optimisation variable at node i:

$$\mathbf{X}_{i+1} - [R_i|M_i]\begin{bmatrix}\mathbf{X}_i\\ \delta\mathbf{v}_i\end{bmatrix} = \tilde{\mathbf{X}}_{i+1} - [R_i|M_i]\begin{bmatrix}\tilde{\mathbf{X}}_i\\ \mathbf{0}\end{bmatrix} \quad (7)$$

- matching of the propagated maneuvered state with the final state:

$$\mathbf{X}_{0,1} + \Delta\mathbf{X}_{1,\delta X_0} + \Delta\mathbf{X}_{1,\delta\mathbf{v}} = \mathbf{X}_{1,1} + \delta\mathbf{X}_1. \quad (8)$$

The problem is purposely handled with linear and quadratic constraints to obtain a convex optimisation formulation, for which convergence and a global minimum are ensured. Slack variables for the δvs magnitude and Mahalanobis distance are introduced to transform the objective function into a linear one and enforce bounds on the Δv and $\delta\mathbf{X}$ magnitude with second-order cone constraints, to finalise the convexification of the problem. Indeed, a quadratic constraint can become a second-order cone with the following variable transformation:

$$\begin{aligned}&\tfrac{1}{2}\mathbf{x}^T A\mathbf{x} + \mathbf{a}^T\mathbf{x} \leq b \iff (w,z,\mathbf{y}) \in \mathcal{Q}_r,\\ &\text{where } \begin{cases}\mathbf{y} = F\mathbf{x}, & Q = FF^T,\\ z = 1, & w = b - \mathbf{a}^T\mathbf{x}\end{cases}\end{aligned} \quad (9)$$

Hence:

$$eq.\ (5) \iff (2v_M, 1, \delta\mathbf{v}_i), \quad (10)$$

and

$$eq.\ (6) \iff \left(2\mathcal{M}, 1, \sqrt{\Lambda^{-1}}Q\delta\mathbf{X}_j\right), \quad (11)$$

where $\Sigma_{(j,j)} = Q\Lambda Q^T$. Once the optimization is completed, the reference trajectory is updated with the optimal maneuver. The accuracy of the final orbit is checked by accurate forward propagation. If constraints are not met to a prescribed accuracy, the procedure is repeated following a standard successive convex optimisation approach, hence modifying eq. (7) introducing an iteration counter k:

$$\mathbf{X}_{i+1}^k - [R_i|M_i]\begin{bmatrix}\mathbf{X}_i^k\\ \delta\mathbf{v}_i^k\end{bmatrix} = \tilde{\mathbf{X}}_{i+1} - [R_i|M_i]\begin{bmatrix}\mathbf{X}_i^{k-1}\\ \delta\mathbf{v}_i^{k-1}\end{bmatrix}. \quad (12)$$

An infeasible flag from the optimization process means that there can't be a maneuver specified by the constraints that can correlate the two objects, and non-correlation is concluded.

Reference trajectories and state transition matrices are developed in C++ using the library Differential Algebra Computing Engine (DACE) [1] and the accurate numerical propagator Accurate Integrator for Debris Analysis (AIDA) [5]. The Matlab interface of the optimizer MOSEK[2] is used to solve the problem with the primal-dual interior-point method for conic quadratic optimization. In principle, any type of coordinates can be chosen for the state representation. However, modified equinoctial elements were chosen because of the easiness to set bounds on the nodes variation and lack of singularities.

3 Keeping a statistical approach

The optimisation finds a deterministic path for this two-boundary value problem. However, the initial and final deviations hold a statistical meaning: the further from the mean states the final solution is, the

[1] https://github.com/dacelib/dace
[2] http://docs.mosek.com/9.0/toolbox/index.html

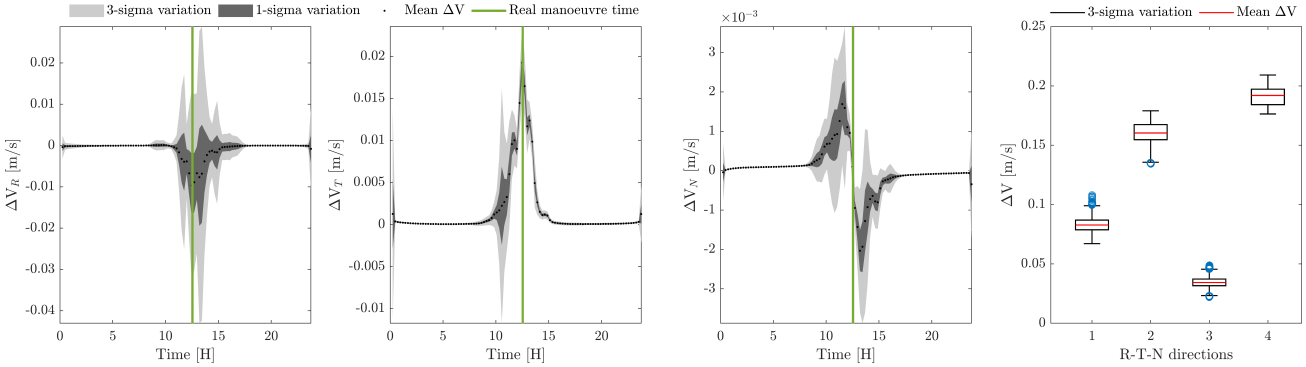

Figure 2: Manoeuvre estimation for two states retrieved one week apart for METEOSAT-8. An East-West station keeping (EWSK) manoeuvre is estimated and statistical properties are retrieved with the conjugate unscented transform (CUT)-4.

less probable the path found is to happen. By simply constraining the initial and final deviations to be less than a value as in eq. (6), the optimiser will see the deviations as "free propellant" hence taking full advantage of them, but actually creating the least probable path. For this reason, ΔX_0 and ΔX_1 cannot be determined within the optimisation but need to be determined beforehand. The fourth order CUT [6] was chosen to do so: by running the optimisation N^2+2N+1 times, where $N=12$ is the dimension of the problem, it is possible to reconstruct a-posteriori the first four momenta of the final distribution, thus making it possible to analyse the effect of uncertainty in the states on the overall maneuver existence and estimation. Sigma points drawn from the initial and final covariance bound the initial and final deviations, so that the constraint in eq. (6) is substituted by:

$$\begin{bmatrix}\delta\mathbf{X}_{0,0}\\ \delta\mathbf{X}_{1,1}\end{bmatrix}_i = \Delta\mathbf{X}^{12x1}_{CUT4,i} \quad i\in\left\{1,\dots,N^2+2N+1\right\}. \tag{13}$$

4 Example: METEOSAT EWSK manoeuvre

To test the optimisation and statistical handling of the uncertainty, a manoeuvre is here reconstructed following the availability of two states with covariances from EUMETSAT weekly newsletter. The data pot also includes the type of manoeuvre and manoeuvre time, but not the profile. Given the long window of time between the two available states, a filter is initially applied to only consider one day where to look for a manoeuvre. To do so, the two states are forward and backward propagated to find the instant in time where they were the closest, and a symmetric 1-day window is considered around that point. Figure 2 shows the manoeuvre time-profile in R, T, and N and the boxplot of the manoeuvres magnitude per components (1-2-3) and overall (4) in the right plot. A clear manoeuvre is visible in the tangential direction, where the 3σ uncertainty is well above zero. Preliminary results are encouraging, but further testing is necessary to make sure that all regimes and manoeuvre types can be handled with successive convexification.

5 Acknowledgments

The work presented is supported by AOARD under Grant FA2386-21-1-4115.

References

[1] L. Pirovano, D. Santeramo, R. Armellin, P. Di Lizia, and A. Wittig, "Probabilistic data association: the orbit set." *Celestial Mechanics and Dynamical Astronomy*, vol. 132, no. 2, p. 15, 2020.

[2] L. Pirovano, R. Armellin, J. Siminski, and T. Flohrer, "Differential algebra enabled multi-target tracking for too-short arcs," *Acta Astronautica*, vol. 182, pp. 310–324, 2021. [Online]. Available: https://www.sciencedirect.com/science/article/pii/S0094576521000977

[3] K. Hill, K. Alfriend, and C. Sabol, "Covariance-based uncorrelated track association," in *AIAA/AAS Astrodynamics Specialist Conference and Exhibit*, 2008, p. 7211.

[4] J. A. Siminski, O. Montenbruck, H. Fiedler, and T. Schildknecht, "Short-arc tracklet association for geostationary objects," *Advances in Space Research*, vol. 53, pp. 1184–1194, Apr. 2014.

[5] A. Morselli, R. Armellin, P. Di Lizia, F. Bernelli-Zazzera, E. Salerno, G. Bianchi, S. Montebugnoli, A. Magro, and K. Z. Adami, "Orbit Determination of Space Debris Using a Bi-Static Radar Configuration with a Multiple-Beam Receiver," *Proceedings of the International Astronautical Congress, IAC*, pp. 1–11, 2014.

[6] "Conjugate unscented transformation: Applications to estimation and control," *Journal of Dynamic Systems, Measurement and Control, Transactions of the ASME*, vol. 140, no. 3, Mar. 2018.